

Article

Improving the Forecasts of Surface Latent Heat Fluxes and Surface Air Temperature in the GRAPES Global Forecast System

Miaoling Liang¹, Xing Yuan^{2,3,*}  and Wenyan Wang^{2,3}

- ¹ CMA Earth System Modeling and Prediction Centre (CEMC), China Meteorological Administration, Beijing 100081, China; liangml@cma.cn
- ² Key Laboratory of Hydrometeorological Disaster Mechanism and Warning of Ministry of Water Resources, Nanjing University of Information Science and Technology, Nanjing 210044, China
- ³ School of Hydrology and Water Resources, Nanjing University of Information Science and Technology, Nanjing 210044, China
- * Correspondence: xyuan@nuist.edu.cn

Abstract: The GRAPES (Global/Regional Assimilation and Prediction System) global medium-range forecast system (GRAPES_GFS) is a new generation numerical weather forecast model developed by the China Meteorological Administration (CMA). However, the forecasts of surface latent heat fluxes and surface air temperature have systematic biases, which affect the forecasts of atmospheric dynamics by modifying the lower boundary conditions and degrading the application of GRAPES_GFS since the 2 m air temperature is one of the key components of weather forecast products. Here, we add a soil resistance term to reduce soil evaporation, which ultimately reduces the positive forecast bias of the land surface latent heat flux. We also reduce the positive forecast bias of the ocean surface latent heat flux by considering the effect of salinity in the calculation of the ocean surface vapor pressure and by adjusting the parameterizations of roughness length for the exchanges in momentum, heat, and moisture between the ocean surface and atmosphere. Moreover, we modify the parameterization of the roughness length for the exchanges in heat and moisture between the land surface and atmosphere to reduce the cold bias of the nighttime 2 m air temperature forecast over areas with lower vegetation height. We also consider the supercooled soil water to reduce the warm forecast bias of the 2 m air temperature over northern China during winter. These modified parameterizations are incorporated into the GRAPES_GFS and show good performance based on a set of evaluation experiments. This paper highlights the importance of the representations of the land/ocean surface and boundary layer processes in the forecasting of surface heat fluxes and 2 m air temperature.

Keywords: GRAPES_GFS; latent heat flux; 2 m air temperature; surface processes; boundary layer



Citation: Liang, M.; Yuan, X.; Wang, W. Improving the Forecasts of Surface Latent Heat Fluxes and Surface Air Temperature in the GRAPES Global Forecast System. *Atmosphere* **2023**, *14*, 1241. <https://doi.org/10.3390/atmos14081241>

Academic Editors: Edoardo Bucignani and Andrea Mastellone

Received: 10 July 2023

Revised: 31 July 2023

Accepted: 1 August 2023

Published: 2 August 2023



Copyright: © 2023 by the authors. Licensee MDPI, Basel, Switzerland. This article is an open access article distributed under the terms and conditions of the Creative Commons Attribution (CC BY) license (<https://creativecommons.org/licenses/by/4.0/>).

1. Introduction

A global model with fully coupled atmosphere, ocean, and land processes is a key component of a numerical weather forecasting system [1]. Currently, there are three main types of weather forecasting systems: global medium-range forecast system, regional mesoscale short-term forecast system, and local convective-scale nowcast system. The global medium-range forecast system is the core of the operational weather forecast system, providing boundary conditions and background information for regional and local weather forecasts. The development of global medium-range weather forecast models has largely contributed to the improvement of worldwide numerical forecasting.

The Global/Regional Assimilation and Prediction Enhanced System (GRAPES) [2] is a new-generation numerical weather prediction model developed by China Meteorological Administration. After nearly 10 years of research and development, the GRAPES global

medium-range ensemble forecast system (GRAPES_GFS) became operational in 2018 [3]. While the atmospheric processes have been reasonably represented by the GRAPES_GFS with advanced physical parameterizations, increased model resolution, and state-of-the-art data assimilation techniques, the representations of surface processes for the land and ocean have received less attention. It is known that the degree of atmospheric response to surface state anomalies is closely related to local boundary layer characteristics, surface heat, and moisture conditions with strong spatial and temporal heterogeneity [4,5]. Due to different surface states, the exchanges in heat, water vapor, and momentum between the surface and the atmosphere are also different, resulting in a variety of different weather conditions [6], especially for extreme weather such as heatwaves [7] and droughts [8,9].

Koster et al. [10] conducted a set of global land–atmospheric coupling experiments using 12 atmospheric models and found that the key factor affecting land–atmospheric coupling is the latent heat flux. Surface flux anomalies caused by soil moisture anomalies affect the development of the boundary layer and the water vapor content in the atmosphere, thus leading to changes in precipitation [11,12]. The observed greening in China caused significant summer cooling and enhanced the summer monsoon precipitation in North China [13]. Qi et al. [14] illustrated that the maximum positive anomaly of precipitation over the eastern Tibetan Plateau lags the warmest surface soil temperature by one phase at the quasi-biweekly timescale, indicating that the warming surface soil temperature could also enhance the subseasonal precipitation. Besides the mean conditions, soil moisture also affects daily maximum and minimum temperature by influencing daytime surface energy distribution and nighttime surface emissivity, with the decrease in soil moisture leading to an increase in daily maximum and minimum temperature [15–17].

The physical parameterizations of GRAPES_GFS have been improved in recent years [18–21]. For instance, Yang et al. [22] showed that the simulation of a stable boundary layer can be improved by incorporating GABLS2 parameterization. The Common Land Model (CoLM) [23] was also coupled into the GRAPES_GFS model, with comprehensive representations of surface and energy exchanges between surface and atmosphere. However, a few systematic biases related to surface processes still exist in GRAPES_GFS. For instance, there are obvious positive biases of latent heat fluxes over land and ocean surfaces as compared with ERA-Interim reanalysis (will be shown in the results section), which is related to the parameterization of evaporation. Over land areas, evaporation consists of soil evaporation, canopy evaporation, and vegetation transpiration. Detailed diagnosis should be performed to investigate the bias in modeling these ET components, which are closely related to soil moisture dynamics and vegetation processes. Over oceans, evaporation is mainly related to radiation, vapor pressure deficit, and the parameterizations of roughness lengths for momentum, temperature, and humidity. These parameterizations may also affect the calculation of 2 m air temperature over the land surface. The soil water processes may also affect temperature calculation over land. For instance, there are liquid soil water even under freezing point, neglecting such process may lead to warm bias over specific regimes, such as northern China during winter.

In this paper, we aim to tackle these shortcomings and improve the corresponding parameterizations of GRAPES_GFS and evaluate the effects of the improved parameterizations on the forecasts of latent heat fluxes over land and ocean, as well as the 2 m air temperature at global and regional scales. Section 2 describes the model parameterizations and experimental design, and Section 3 presents the evaluation results. Conclusions and discussion are presented in Section 4.

2. Model Parameterizations and Experimental Design

2.1. GRAPES_GFS

GRAPES_GFS is a global medium-range weather forecast model that includes an atmospheric model, a land surface model, a simple ocean flux model with fixed sea surface temperature (SST) at the beginning of the forecast, and a variational data assimilation system [24]. The atmospheric model is a nonhydrostatic model, with a spatial discretization

of the staggered Arakawa C grid and a temporal discretization of two-time-level semi-implicit semi-Lagrangian scheme [25]. The atmospheric model has 87 levels, with a model top of 0.1 hPa. The physical schemes of GRAPES_GFS consist of the RRTMG short-wave and long-wave radiation parameterizations, a double-moment cloud microphysical scheme, the NSAS shallow and deep cumulus convection parameterizations, the MRF planetary boundary layer scheme, and the CoLM land surface scheme [3]. The CoLM [26] calculates the soil water and temperature dynamics in different soil layers, the accumulation and melting of snow, surface and subsurface runoff, as well as the latent and sensible heat fluxes over both land and ocean. It was developed from NCAR CLM [23] but introduced the two-big-leaf model for calculating the exchanges in energy, water, and carbon between land surface and atmosphere and incorporated high-resolution soil data [26].

2.2. Improved Parameterizations for the Estimation of Latent Heat Flux

The surface latent heat flux is the energy of evaporation. GRAPES_GFS calculates evaporation over land by using the parameterizations of surface soil evaporation, vegetation transpiration, and canopy evaporation. GRAPES_GFS also calculates evaporation over ocean by using a simple ocean flux scheme. To address the issue of overestimated soil evaporation from the CoLM model, a soil resistance term that limits excessive evaporation was added during the development of NCAR CLM 3.5 [27]. It also proved to be useful in improving the Conjunctive Surface and Subsurface Process model (CSSP) [28]. Therefore, we also added such soil resistance term (R_s) [27,28] into GRAPES_GFS as follows:

$$R_s = \exp(8.206 - 4.255S_1) \quad (1)$$

where S_1 is the relative soil moisture of the surface soil layer. Note that this is an additional resistance for the calculation of soil evaporation, and the resistance is larger if the surface soil is drier.

The transfer coefficient for moisture and heat that controls the total heat flux being transported into atmosphere is more sensitive to roughness length for moisture/heat than the stability function [29]. In original GRAPES_GFS, the roughness lengths for momentum (Z_{0M}), heat (Z_{0T}) and moisture (Z_{0Q}) over ocean are expressed as follows:

$$z_{0M} = 0.11 \frac{\nu}{u_*} + \alpha \frac{u_*^2}{g} \quad (2)$$

$$z_{0T} = z_{0Q} = 2.67(R_e^*)^{1/4} - 2.57 \quad (3)$$

$$R_e^* = \frac{u_* z_{0M}}{\nu} \quad (4)$$

where α is the Charnock coefficient with the constant value of 0.013, ν is the kinematic viscosity dependent on SST, u_* is the friction velocity, g is acceleration of gravity. To reduce the positive biases of latent heat fluxes, we modified the calculation of roughness lengths for temperature and humidity over sea by following the ECMWF model [30] as follows:

$$z_{0T} = 0.40 \frac{\nu}{u_*} \quad (5)$$

$$z_{0Q} = 0.62 \frac{\nu}{u_*} \quad (6)$$

and we modified the Charnock coefficient for the calculation of the roughness length for momentum by considering the wind speed effect [31] as follows:

$$\alpha = \begin{cases} 0.011, & U \leq 10 \text{ m/s} \\ 0.011 + 0.007(U - 10)/8, & 10 < U < 18 \text{ m/s} \\ 0.018, & U \geq 18 \text{ m/s} \end{cases} \quad (7)$$

In addition, the original GRAPES_GFS/CoLM used the saturated specific humidity at SST as the boundary condition for vapor pressure calculation, which ignored the salinity effect and overestimated the latent heat flux over ocean due to the overestimation of the pressure gradient between ocean and atmosphere. Therefore, we modified the calculation of specific humidity at ocean surface as follows:

$$q_s = 0.98q_{sat}(SST) \tag{8}$$

2.3. Improved Parameterization for the Estimation of 2 m Air Temperature

The original GRAPES_GFS/CoLM did not distinguish the roughness lengths for the exchanges in momentum, heat, and moisture over land surface, which resulted in the cold bias for the forecast of nighttime 2 m air temperature. Here, we adopted the calculation of roughness length for the heat and moisture exchanges as in ECMWF IFS, where 1% of the roughness length for momentum exchange is used for estimating the roughness lengths for the heat and moisture exchanges for vegetation with low height, while the original momentum roughness length is used for heat and moisture roughness lengths for tall vegetation.

In order to reduce the warm bias for the forecast of 2 m air temperature over cold regions during winter, we considered the supercooled water in the calculation of soil water dynamics, which allows for the coexistence of liquid soil water with solid soil water for the temperatures below the freezing point [32,33]. The supercooled water is estimated as follows:

$$w_{liq,max,i} = \Delta z_i \theta_{sat,i} \left[\frac{10^3 L_f (T_f - T_i)}{g T_i \psi_{sat,i}} \right]^{-1/B_i} \quad T_i < T_f \tag{9}$$

where $w_{liq,max,i}$ is the maximum liquid water content when the soil temperature T_i is below the freezing point T_f in the i th soil layer, L_f is the latent heat of fusion, and g is the gravitational acceleration. When $T_i < T_f$ and $w_{liq,i} > w_{liq,max,i}$, icing occurs. The ice content at the next time step is calculated as follows [34]:

$$w_{ice,i}^{n+1} = \left\{ \begin{array}{l} \min \left(w_{liq,i}^n + w_{ice,i}^n - w_{liq,max,i}^n, w_{ice,i}^n - \frac{H_i \Delta t}{L_f} \right) \quad w_{liq,i}^n + w_{ice,i}^n \geq w_{liq,max,i}^n \\ 0 \quad w_{liq,i}^n + w_{ice,i}^n < w_{liq,max,i}^n \end{array} \right\} \tag{10}$$

where H_i is the energy required for the temperature change from T_i to T_f ($H_i < 0$), and part of the energy (H_{i^*}) is not released during the icing process but is used to cool the soil, which is expressed as

$$H_{i^*} = H_i - \frac{L_f (w_{ice,i}^n - w_{ice,i}^{n+1})}{\Delta t} \tag{11}$$

The introduction of supercooled soil water allows the soil temperature with liquid water lower than freezing point, which reduces the warm bias of winter 2 m air temperature forecasts.

2.4. Experimental Design

To evaluate the performance of the modified GRAPES_GFS, we carried out numerical experiments which incorporated the modified parameterizations gradually:

- (1) EXP1 experiment by using GRAPES_GFS with modified parameterizations of soil evaporation and ocean surface roughness length, where the 24 h forecasts started from each day during 1–31 July 2016;
- (2) EXP2 experiment by using GRAPES_GFS with modified parameterizations from EXP1, and land surface roughness lengths for the exchanges in heat and moisture, salinity-related ocean surface vapor pressure, where the 24 h forecasts started from each day during 1 March–15 April 2019;

- (3) EXP3 experiment by using GRAPES_GFS with modified parameterizations from EXP1 and EXP2, as well as the supercooled soil water, where the 24 h forecasts started from each day during 1–31 January 2016;
- (4) CTL experiments are the same as EXP1–EXP3 but use the original GRAPES_GFS without any modifications in the surface parameterizations mentioned above.
- (5) To evaluate the performance of precipitation forecasts, we use the model version same as EXP3 to perform 24 h forecasts during 16 June–30 September 2019. This experiment is denoted as EXP4.

All the experiments were initialized by using the ERA-Interim reanalysis for atmospheric and land surface variables and the SST from NOAA/OISST. The spatial resolution for the forecasts is 0.25 degrees. These experiments were used to evaluate the model performances during different seasons where model had obvious biases.

3. Results

3.1. Evaluation of the GRAPES_GFS Forecasts of Latent Heat Fluxes

Given that in situ observations of surface latent heat fluxes are very limited in a few FLUXNET stations, we use latent heat estimation from the ERA-Interim reanalysis data as a proxy for global model evaluation. Although reanalysis is also a model product, we believe the observation assimilation of other variables could help constrain the simulation of surface latent heat fluxes. Figure 1a shows that the surface latent heat fluxes predicted in the GRAPES_GFS CTL experiment are larger than the ERA-Interim reanalysis over most tropical and mid-latitude areas, especially for tropical oceans, western and central Africa, Amazon, eastern China, India, southeastern and northern Asia, Europe, the eastern part of North America, and Central America. The overestimation of surface latent heat fluxes could be related to systematic biases of cloud and radiation modeling. The GRAPES_GFS was found to underestimate the cloud cover and thus overestimate surface radiation [25], which could lead to the overestimation of surface fluxes. Besides cloud-radiation issues, the surface processes could also contribute to the overestimation of surface latent heat fluxes and, in turn, affect cloud and radiative processes through land–atmospheric coupling. Here we show that after considering the soil resistance, the surface latent heat flux is reduced over most land areas with positive biases, including western Africa, eastern China, and North America (Figure 1b). This indicates that the improved GRAPES_GFS effectively reduces the positive forecast bias of the land surface latent heat flux.

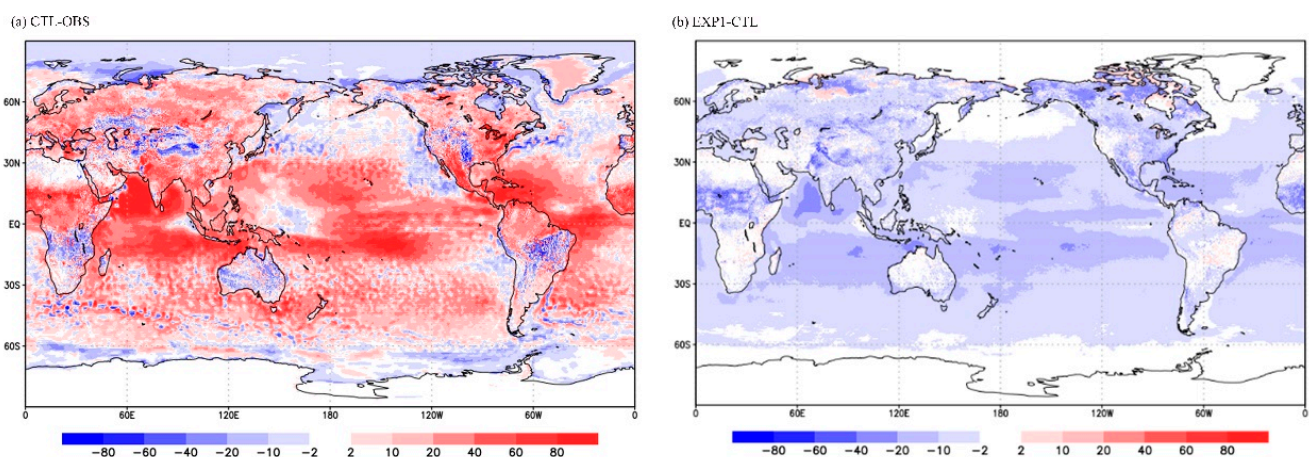


Figure 1. Comparison of the 24 h forecasts of latent heat fluxes (W/m^2) averaged in July 2016. The left panel (a) is the difference between the original GRAPES_GFS experiment (CTL) and ERA interim reanalysis, and the right panel (b) is the difference between the improved GRAPES_GFS experiment (EXP1; with modifications in the parameterizations of surface latent heat fluxes) and the CTL experiment. The 24 h forecasts started from each day during 1–31 July 2016.

In terms of the systematic bias of the ocean surface latent heat flux, sensitivity tests were conducted for changing wind speed and specific humidity. Reducing ocean surface wind speed significantly reduced the ocean surface latent heat flux, but there was no systematic bias of the GRAPES_GFS ocean surface wind speed compared with reanalysis (not shown). Therefore, the bias of the ocean's latent heat flux was not caused by the wind speed bias. The GRAPES_GFS model is very sensitive to the specific humidity of the ocean surface, and increasing the specific humidity can reduce the latent heat flux. Moreover, the specific humidity of the near-surface atmosphere predicted by GRAPES_GFS is significantly drier over tropical oceans as compared with ERA-Interim reanalysis. Therefore, it is assumed that the excessive latent heat flux at the ocean surface is mainly due to the dryness of the near-surface atmosphere. Driven by the ocean surface humidity field of ERA-Interim reanalysis, we can obtain more reasonable latent heat fluxes in an offline mode, but there are still some positive biases. Therefore, we believe there are systematic biases in the ocean flux calculation in GRAPES_GFS.

One of the reasons for the positive bias in latent heat flux over oceans is that the ocean surface vapor pressure of GRAPES_GFS is equivalent to the saturated vapor pressure without considering the effect of salinity. Thus, it increases the pressure gradient between the bottom atmosphere and the ocean surface, which inevitably leads to a large latent heat bias. Therefore, we refer to the ECMWF IFS model and consider the effect of salinity in the calculation of the ocean surface vapor pressure, which is about 98% of the saturated vapor pressure. However, this treatment also slightly reduces the positive bias of the latent heat flux at the ocean surface (not shown). After improving the parameterizations of roughness lengths for the exchanges in momentum, heat, and moisture, a set of 24 h hindcasts during 1–31 July 2016 show that the positive biases of latent heat fluxes can be significantly reduced over the ocean (Figure 1b). The reductions can reach 10–20 W/m² over specific tropical ocean areas.

The correction of surface latent heat fluxes also improves the forecasts of atmospheric water vapor content at different pressure levels (Figure 2). As compared with ERA-Interim reanalysis, there are positive biases in the GRAPES_GFS CTL experiment for the atmospheric water vapor forecasts from surface to 400–600 hPa between 60 S–60 N (Figure 2a). The positive biases are more significant in the subtropical Northern Hemisphere than in the subtropical Southern Hemisphere (Figure 2a), which is consistent with the results for the positive biases of latent heat fluxes. With modified parameterizations of soil evaporation and ocean surface roughness length, the GRAPES_GFS EXP1 experiment reduced the positive biases of low-level atmospheric water vapor content significantly, especially from surface to 850 hPa between 30 S–60 N (Figure 2b). Again, the improvement in the forecasts of atmospheric water vapor content is more significant in Northern Hemisphere.

3.2. Evaluation of the GRAPES_GFS Forecasts of 2 m Air Temperature

Considering that the 2 m air temperature is the most critical information provided by routine weather forecasts, we also assessed the GRAPES_GFS performance in this regard. Figure 3 shows a snapshot of the 2 m air temperature forecast over China on 11 March 2019. As compared with the 2 m air temperature observations at national weather stations, the GRAPES_GFS forecasts have warm biases at 00 UTC over most stations except for Huang-Huai-Hai plain and Sichuan province (Figure 3a) and large cold biases at 12 UTC across China (Figure 3c). Since the 2 m air temperature is determined by the gradient of land skin temperature and bottom atmospheric temperature, we carefully analyzed each component affecting the 2 m air temperature calculation and found that the nighttime 2 m air temperature is much lower than the bottom atmospheric temperature and land skin temperature, which suggests that GRAPES_GFS underestimated the canopy temperature at night. In addition, we noted that GRAPES_GFS did not take into account the difference between the heat/moisture roughness length and the momentum roughness length, which are actually very different [35]. Therefore, in this paper, we adopted the thermal roughness length calculation method of ECMWF IFS to correct the unreasonably

low value of nighttime canopy temperature and finally reduced the cold biases of nighttime 2 m air temperature in eastern China (Figure 3d), although the biases for daytime 2 m air temperature did not change (Figure 3b). We extend the analysis from China to the globe and from the forecasts within the first 24 h to 120 h. Figure 4 shows that the new parameterizations effectively increased the local nighttime temperature around the globe, and the increases are consistent over forecast lead times.

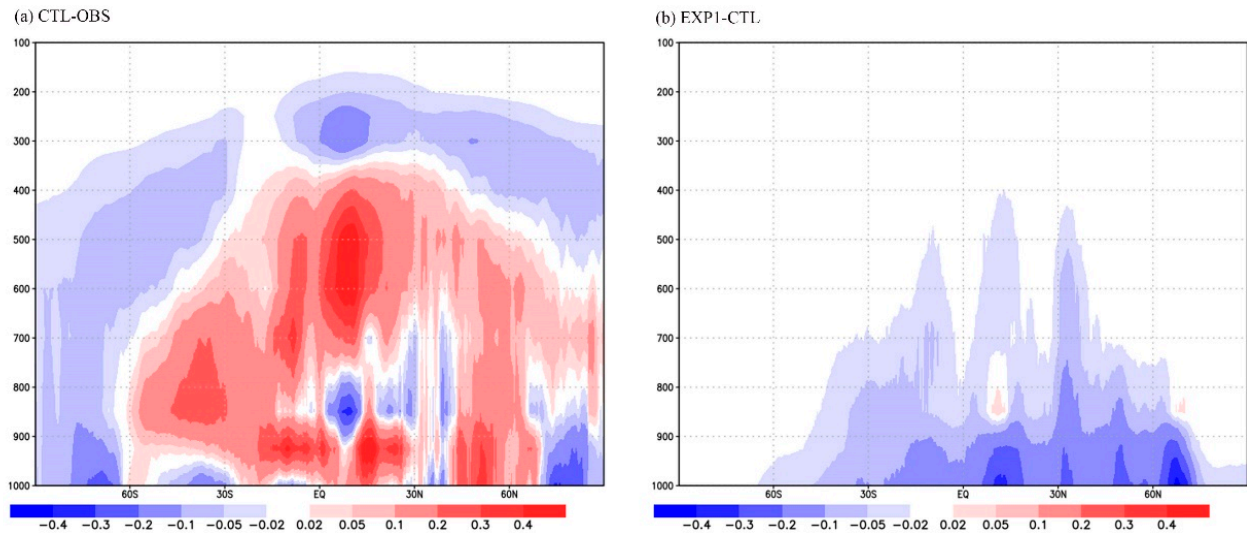


Figure 2. The same as Figure 1, but for the latitudinal averages of atmospheric column water vapor content (g/kg) for the 24 h forecasts during 1–31 July 2016.

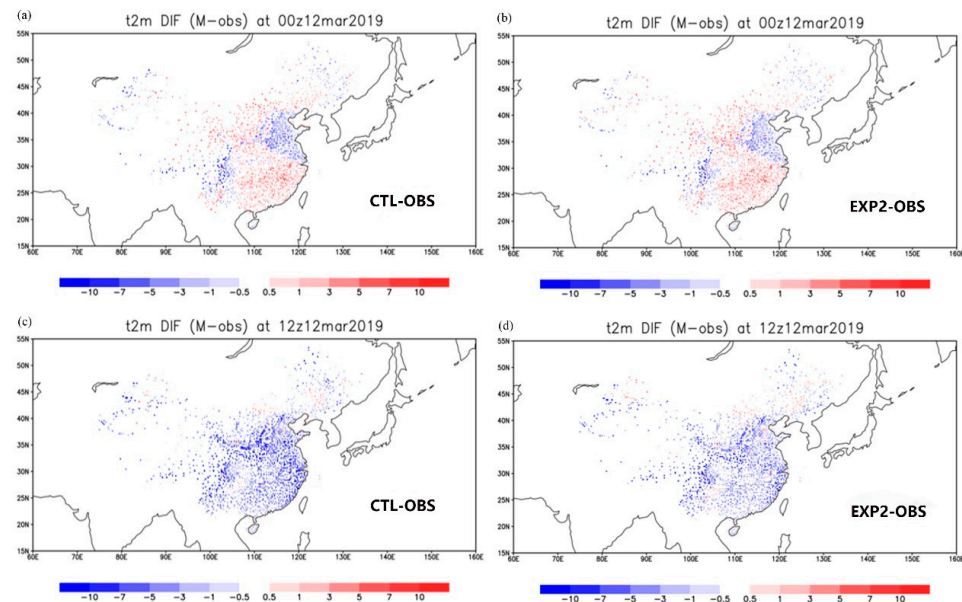


Figure 3. Biases for the 2 m air temperature forecasts ($^{\circ}\text{C}$) at 2000+ weather stations in China. The forecasts started from 12 UTC on 11 March 2019, with the lead times of 12 h (top panels, a,b) and 24 h (bottom panels, c,d). The left panels (a,c) are for the biases of CTL experiment, and the right panels (b,d) are for the biases of improved GRAPES_GFS experiment (EXP2; with modifications in the parameterizations of soil evaporation and roughness length).

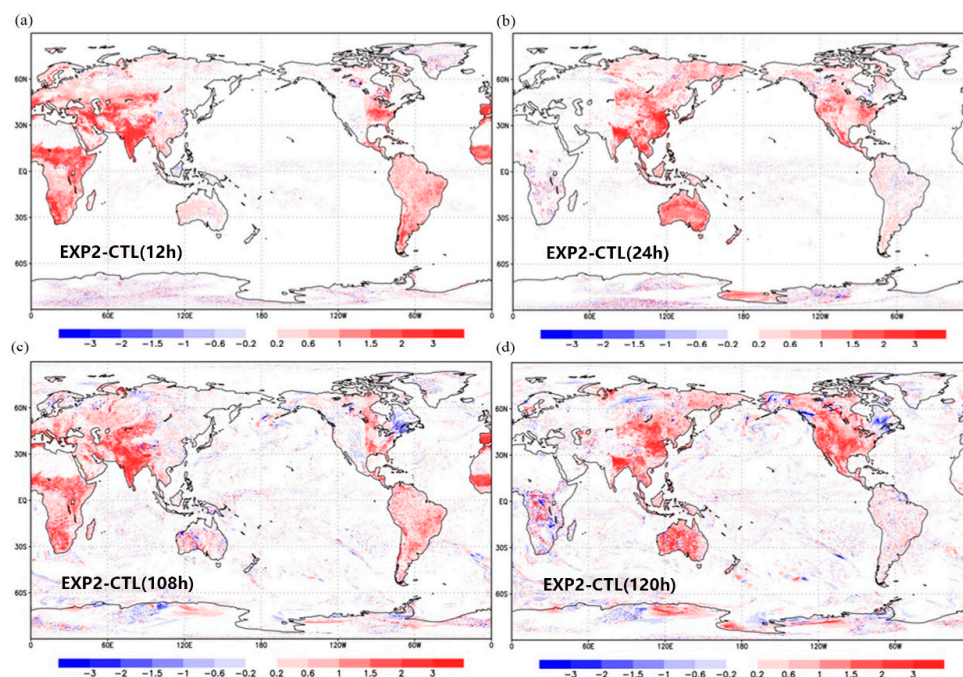


Figure 4. Differences in 2 m air temperature ($^{\circ}\text{C}$) forecasts between improved GRAPES_GFS experiment (EXP2; with modifications in the parameterizations of soil evaporation and roughness length) and CTL experiment at with different forecast lead times. The forecasts started at 12 UTC on 11 March 2019. (a–d) are the differences for lead times of 12 hours, 24 hours, 108 hours and 120 hours, respectively.

Besides the snapshot on 11 March 2019, we also calculated the root mean squared errors (RMSEs) for nighttime 2 m air temperature forecasts averaged across 2000+ weather stations from March 1 to April 15 in 2019 (Figure 5). The fluctuations of RMSEs are similar between CTL and EXP2 experiments, but the latter has 1°C less RMSEs (Figure 5). When analyzing the diurnal cycle of 2 m temperature, we noticed that GRAPES_GFS forecast temperature over northern China in the winter was too warm. Our further analysis showed that this was due to the fact that the model only considered two types of soil water phases when determining the solid or liquid state, i.e., whether the soil temperature was below freezing point or not. Here, we introduced the parameterization of supercooled soil water to consider liquid water existed in the soil for the soil temperature below the freezing point, which allowed the soil temperature to be lower than the freezing point. As a result, the root mean squared error for the 2 m air temperature forecast was reduced (Figure 6).

To explore whether the improvements in the representations of surface processes affect precipitation forecasts, Figure 7 shows the biases for the 24 h precipitation forecasts in CTL and EXP4 experiments. The CTL experiment shows that GRAPES_GFS has overestimations for rainfall frequency if counting all rainfall events (daily rainfall > 0.1 mm) while underestimations for heavy rainfall frequency (daily rainfall > 25 mm). This is similar to most global forecast models, where light rainfalls are usually overestimated and heavy rainfalls are underestimated due to a number of issues, including coarse resolution and deficiencies in the parameterizations of shallow convection and/or deep convection. The reduction in positive biases of latent heat flux forecasts in the GRAPES_GFS model is responsible for the reductions in positive biases of light rainfall forecasts, i.e., those with daily rainfall less than 5 mm (Figure 7). For heavy rainfall, the changes are not obvious, suggesting that other processes instead of surface fluxes are dominant controls of the underestimation.

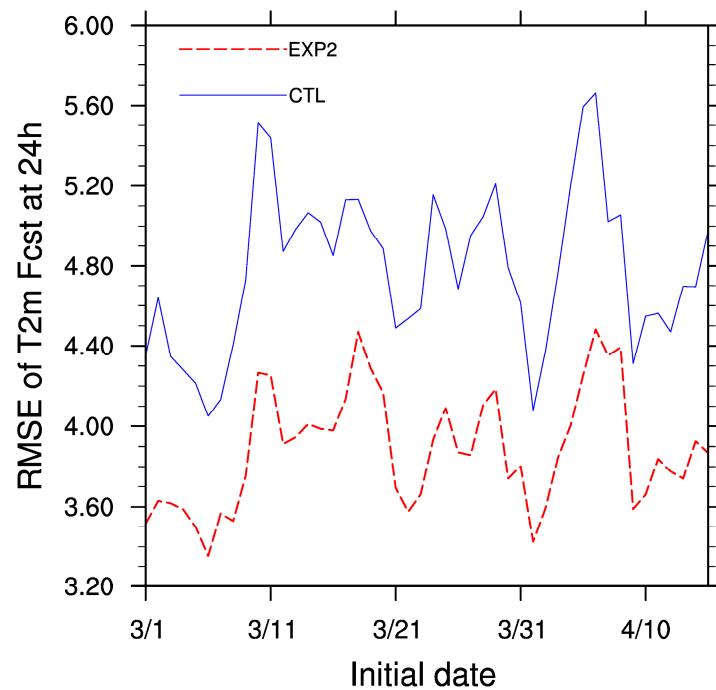


Figure 5. Root mean squared error (RMSE; °C) of 24 h forecasts of 2 m air temperature for CTL experiment and improved GRAPES_GFS experiment (EXP2; with modifications in the parameterizations of soil evaporation and roughness length). The forecasts started at 12 UTC on each day from 1 March 2019 to 15 April 2019. The forecasts were compared with the observations from 2000+ weather stations in China, and the mean RMSEs were shown.

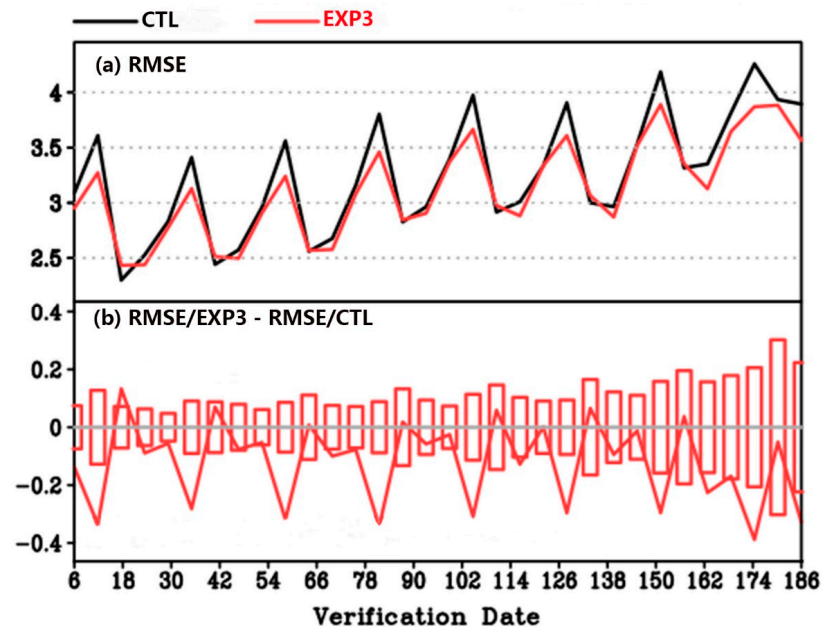


Figure 6. Root mean squared error (RMSE; °C) of 2 m air temperature forecasts over northeastern China with lead times from 6 h to 186 h for CTL experiment and improved GRAPES_GFS experiment (EXP3; with parameterizations of soil evaporation, roughness length and the supercooled soil water). The forecasts started at 12 UTC on each day from 1 January 2016 to 31 January 2016, and RMSE for each forecast lead was calculated. The top panel shows the RMSE for CTL and EXP3, while the bottom panel shows the differences in RMSE between EXP3 and CTL. Negative values in the bottom panel show the reduction of RMSE after improving GRAPES_GFS, and the error reduction is significant if it exceeds the uncertainty with 95% confidence level indicated by the vertical bars.

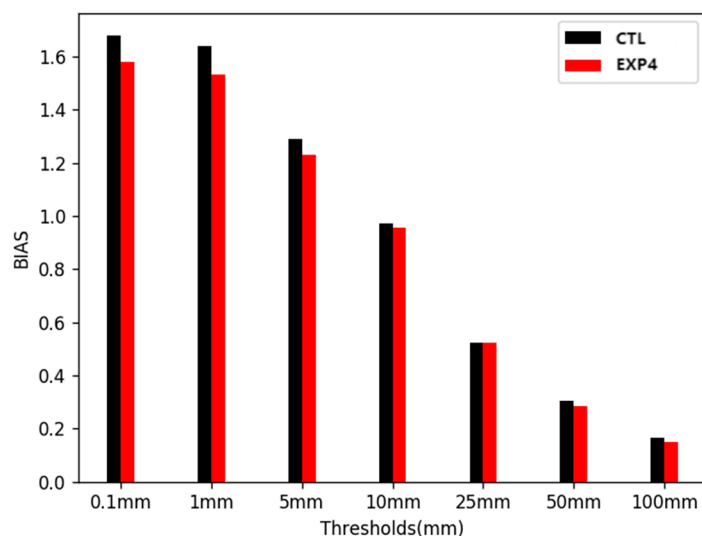


Figure 7. Biases of 24 h precipitation forecasts (mm) started each day from 16 June 2019 to 30 September 2019 for CTL experiment and improved GRAPES_GFS experiment (EXP4; the model version is the same as EXP3, but for forecasts during summer period). The bias was calculated as the ratio of forecast rainfall events over the observed rainfall events, and the values close to 1 suggested un-biased forecasts. The horizontal axis showed the rainfall thresholds, where the events with daily rainfall larger than the threshold were counted. The forecasts were compared with the observations from 2000+ weather stations in China, and the mean biases were shown.

4. Conclusions and Discussion

This paper improves the GRAPES_GFS forecasts of surface latent heat fluxes and 2 m air temperature by adding a soil resistance term in the calculation of soil evaporation, considering the salinity effect in the calculation of ocean surface vapor pressure, distinguishing the roughness length parameterizations for the exchanges in momentum, heat, and moisture, and incorporating the parameterization of supercooled soil water. As a result, the excessive latent heat flux has been reduced over both land surface and ocean surface, and RMSE for 2 m air temperature has also been reduced by 1 °C averaged over national weather observation stations.

This study suggests that a correction for the surface heat flux has a fundamental influence on the dynamics of the near-surface atmosphere even for a numerical weather prediction model, where the forecast error of a critical weather service variable, 2 m air temperature, can be significantly reduced through reasonable modeling of roughness length and soil water and energy dynamics. The importance of ocean and land surface conditions has long been overlooked in weather forecasts because the slow evolutions of oceanic and land surface processes were regarded as having no significant influence on the atmosphere at a synoptic scale. Although the surface processes are emphasized in global models that are targeted for a seamless prediction of weather and climate in recent years, many weather forecast models still treat the ocean surface conditions as constant and the land surface conditions as climatology. In fact, the forecasts of extreme events are closely related to the initial oceanic and land surface conditions [8], and these slowly evolving processes provide critical sources of predictability that can help to extend the current weather forecast limit.

The atmospheric data assimilation of GRAPES_GFS is being mature after decades of development, but the land surface data assimilation of GRAPES_GFS is rather simple. The exchanges between land/ocean and atmosphere are being intensified in a warming climate, where the recent urban heatwaves and marine heatwaves provide strong evidence. The intensity of these extremes might be under-forecast if the local and remote surface-atmosphere interactions are not well represented in global forecast models. Therefore, more attention should be paid to oceanic and land surface processes in developing GRAPES_GFS,

no matter for a seamless prediction or for the early warning of major extreme events under climate change.

Author Contributions: Conceptualization, M.L. and X.Y.; Methodology, M.L.; Software, M.L. and W.W.; Writing—original draft, M.L. and X.Y.; Writing—review and editing, M.L., X.Y. and W.W. All authors have read and agreed to the published version of the manuscript.

Funding: This work was supported by National Key R&D Program of China (2018YFC1505701), National Natural Science Foundation of China (U22A20556), Natural Science Foundation of Jiangsu Province for Distinguished Young Scholars (BK20211540), and the Major Science and Technology Program of the Ministry of Water Resources of China (SKS-2022019).

Data Availability Statement: The GRAPES_GFS data is available upon request.

Conflicts of Interest: The authors declare that they have no known competing financial interest or personal relationships that could have appeared to influence the work reported in this paper.

References

- Bauer, P.; Thorpe, A.; Brunet, G. The Quiet Revolution of Numerical Weather Prediction. *Nature* **2015**, *525*, 47–55. [[CrossRef](#)]
- Chen, D.-H.; Shen, X.-S. Recent Progress on GRAPES Research and Application. *J. Appl. Meteorol. Sci.* **2006**, *17*, 773–777.
- Chen, J.; Li, X.-L. The Review of 10 Years Development of the GRAPES Global/Regional Ensemble Prediction. *Adv. Meteorol. Sci. Technol.* **2020**, *10*, 9–18.
- Betts, A.K.; Ball, J.H.; Beljaars, A.C.M.; Miller, M.J.; Viterbo, P.A. The Land Surface–Atmosphere Interaction: A Review Based on Observational and Global Modeling Perspectives. *J. Geophys. Res. Atmos.* **1996**, *101*, 7209–7225. [[CrossRef](#)]
- Seneviratne, S.I.; Corti, T.; Davin, E.L.; Hirschi, M.; Jaeger, E.B.; Lehner, I.; Orlowsky, B.; Teuling, A.J. Investigating Soil Moisture–Climate Interactions in a Changing Climate: A Review. *Earth-Sci. Rev.* **2010**, *99*, 125–161. [[CrossRef](#)]
- Yu, Y.; Xie, Z.-H. A Simulation Study on Climatic Effects of Land Cover Change in China. *Adv. Clim. Chang. Res.* **2013**, *4*, 117–126. [[CrossRef](#)]
- Zhou, S.; Yuan, X. Upwind Droughts Enhance Half of the Heatwaves over North China. *Geophys. Res. Lett.* **2022**, *49*, e2021GL096639. [[CrossRef](#)]
- Liang, M.; Yuan, X. Critical Role of Soil Moisture Memory in Predicting the 2012 Central United States Flash Drought. *Front. Earth Sci.* **2021**, *9*, 615969. [[CrossRef](#)]
- Yuan, X.; Wang, Y.; Ji, P.; Wu, P.; Sheffield, J.; Otkin, J.A. A Global Transition to Flash Droughts under Climate Change. *Science* **2023**, *380*, 187–191. [[CrossRef](#)]
- Koster, R.D.; Sud, Y.C.; Guo, Z.; Dirmeyer, P.A.; Bonan, G.; Oleson, K.W.; Chan, E.; Verseghy, D.; Cox, P.; Davies, H.; et al. GLACE: The Global Land–Atmosphere Coupling Experiment. Part I: Overview. *J. Hydrometeorol.* **2006**, *7*, 590–610. [[CrossRef](#)]
- Santanello, J.A.; Peters-Lidard, C.D.; Kumar, S.V. Diagnosing the Sensitivity of Local Land–Atmosphere Coupling via the Soil Moisture–Boundary Layer Interaction. *J. Hydrometeorol.* **2011**, *12*, 766–786. [[CrossRef](#)]
- Li, K.; Zhang, J.; Wu, L. Assessment of Soil Moisture–Temperature Feedbacks with the CCSM-WRF Model System Over East Asia. *J. Geophys. Res. Atmos.* **2018**, *123*, 6822–6839. [[CrossRef](#)]
- Yu, L.; Xue, Y.; Diallo, I. Vegetation Greening in China and Its Effect on Summer Regional Climate. *Sci. Bull.* **2021**, *66*, 13–17. [[CrossRef](#)]
- Qi, X.; Yang, J.; Xue, Y.; Bao, Q.; Wu, G.; Ji, D. Subseasonal Warming of Surface Soil Enhances Precipitation over the Eastern Tibetan Plateau in Early Summer. *J. Geophys. Res. Atmos.* **2022**, *127*, e2022JD037250. [[CrossRef](#)]
- Zhang, J.; Wang, W.-C.; Wu, L. Land–Atmosphere Coupling and Diurnal Temperature Range over the Contiguous United States. *Geophys. Res. Lett.* **2009**, *36*, L06706. [[CrossRef](#)]
- Yuan, G.; Zhang, L.; Liang, J.; Cao, X.; Guo, Q.; Yang, Z. Impacts of Initial Soil Moisture and Vegetation on the Diurnal Temperature Range in Arid and Semiarid Regions in China: Effects of Land Surface on Temperature. *J. Geophys. Res. Atmos.* **2017**, *122*, 11568–11583. [[CrossRef](#)]
- He, Y.-L.; Ding, L.; Li, D.-D.; Huang, J.-P.; Li, C.-Y.; Bi, L. Research Review on the Contrast of Land and Ocean Warming Features Under the Global Warming. *J. Arid Meteorol.* **2019**, *37*, 703–712. [[CrossRef](#)]
- Wan, Z.-W.; Wang, J.-J.; Huang, L.-P.; Kang, J.-Q. An Improvement of the Shallow Convection Parameterization Scheme in the GRAPES-Meso. *Acta Meteorol. Sin.* **2015**, *73*, 1066–1079. [[CrossRef](#)]
- Huang, W.; Zhang, X.; Bao, J.-W.; Chen, B.-D. Implementation and Improvement of the GFS Physics Package in the GRAPES Regional Model: Single Column Experiments. *Chin. J. Atmos. Sci.* **2018**, *42*, 1219–1234. [[CrossRef](#)]
- Zhao, B.; Zhang, B. Application of a Bias Correction Scheme for 2-Meter Temperature Levels over Complex Terrain. *Trans. Atmos. Sci.* **2018**, *41*, 657–667. [[CrossRef](#)]
- Peng, Y.; Wang, H.; Hou, M.; Jiang, T.; Zhang, M.; Zhao, T.; Che, H. Improved Method of Visibility Parameterization Focusing on High Humidity and Aerosol Concentrations during Fog–Haze Events: Application in the GRAPES_CAUCE Model in Jing-Jin-Ji, China. *Atmos. Environ.* **2020**, *222*, 117139. [[CrossRef](#)]

22. Yang, J.-L.; Shen, X.-S.; Chen, J. Objective Evaluation of PBL Parameterization Scheme in GRAPES Based on GABLS2. *Meteorol. Sci. Technol.* **2019**, *47*, 276–281.
23. Dai, Y.; Zeng, X.; Dickinson, R.E.; Baker, I.; Bonan, G.B.; Bosilovich, M.G.; Denning, A.S.; Dirmeyer, P.A.; Houser, P.R.; Niu, G.; et al. The Common Land Model. *Bull. Am. Meteorol. Soc.* **2003**, *84*, 1013–1024. [[CrossRef](#)]
24. Ma, Z.; Zhao, C.; Gong, J.; Zhang, J.; Li, Z.; Sun, J.; Liu, Y.; Chen, J.; Jiang, Q. Spin-up Characteristics with Three Types of Initial Fields and the Restart Effects on the Forecast Accuracy in GRAPES Global Forecast System. *Geosci. Model Dev.* **2021**, *14*, 205–221. [[CrossRef](#)]
25. Ma, Z.; Liu, Q.; Zhao, C.; Shen, X.; Wang, Y.; Jiang, J.H.; Li, Z.; Yung, Y. Application and evaluation of an explicit prognostic cloud-cover scheme in GRAPES global forecast system. *J. Adv. Model. Earth Syst.* **2018**, *10*, 652–667. [[CrossRef](#)]
26. Dai, Y.; Dickinson, R.E.; Wang, Y.P. A two-big-leaf model for canopy temperature, photosynthesis, and stomatal conductance. *J. Clim.* **2004**, *17*, 2281–2299. [[CrossRef](#)]
27. Oleson, K.W.; Niu, G.-Y.; Yang, Z.-L.; Lawrence, D.M.; Thornton, P.E.; Lawrence, P.J.; Stöckli, R.; Dickinson, R.E.; Bonan, G.B.; Levis, S.; et al. Improvements to the Community Land Model and Their Impact on the Hydrological Cycle: COMMUNITY LAND MODEL HYDROLOGY. *J. Geophys. Res. Biogeosci.* **2008**, *113*, G01021. [[CrossRef](#)]
28. Yuan, X.; Liang, X.-Z. Evaluation of a Conjunctive Surface–Subsurface Process Model (CSSP) over the Contiguous United States at Regional–Local Scales. *J. Hydrometeorol.* **2011**, *12*, 579–599. [[CrossRef](#)]
29. Chen, F.; Janjić, Z.; Mitchell, K. Impact of Atmospheric Surface-Layer Parameterizations in the New Land-Surface Scheme of the NCEP Mesoscale Eta Model. *Bound.-Layer Meteorol.* **1997**, *85*, 391–421. [[CrossRef](#)]
30. Beljaars, A.C.M. The Parametrization of Surface Fluxes in Large-Scale Models under Free Convection. *Q. J. R. Meteorol. Soc.* **1995**, *121*, 255–270. [[CrossRef](#)]
31. Fairall, C.W.; Bradley, E.F.; Hare, J.E.; Grachev, A.A.; Edson, J.B. Bulk Parameterization of Air–Sea Fluxes: Updates and Verification for the COARE Algorithm. *J. Clim.* **2003**, *16*, 571–591. [[CrossRef](#)]
32. Niu, G.-Y.; Yang, Z.-L. Effects of Frozen Soil on Snowmelt Runoff and Soil Water Storage at a Continental Scale. *J. Hydrometeorol.* **2006**, *7*, 937–952. [[CrossRef](#)]
33. Oleson, K.W.; Niu, G.-Y.; Yang, Z.-L.; Lawrence, D.M.; Thornton, P.E.; Lawrence, P.J.; Stockli, R.; Dickinson, R.E.; Bonan, G.B.; Levis, S. *CLM3.5 Documentation*; National Center for Atmospheric Research: Boulder, CO, USA, 2007.
34. Oleson, K.W.; Dai, Y.-J.; Bonan, B.; Bosilovich, M.; Dickinson, R.; Dirmeyer, P.; Hoffman, F.; Houser, P.; Houser, P.; Levis, S.; et al. *Technical Description of the Community Land Model (CLM)*; (No. NCAR/TN-461+STR); University Corporation for Atmospheric Research: Boulder, GA, USA, 2004. [[CrossRef](#)]
35. Garratt, J.R. *The Atmospheric Boundary Layer*; Cambridge Atmospheric and Space Science Series; Cambridge University Press: Cambridge, UK, 1992.

Disclaimer/Publisher’s Note: The statements, opinions and data contained in all publications are solely those of the individual author(s) and contributor(s) and not of MDPI and/or the editor(s). MDPI and/or the editor(s) disclaim responsibility for any injury to people or property resulting from any ideas, methods, instructions or products referred to in the content.